JOURNAL OF
Optical Communications
and Networking

Experimental real-time GbE MIMO FSO under fog conditions with software defined GNU Radio platform-based adaptive switching

Zun Htay,[1,*] Carlos Guerra-Yánez,[2] Zabih Ghassemlooy,[1] Stanislav Zvanovec,[2] Mojtaba Mansour Abadi,[1] and Andrew Burton[3]

[1]Optical Communications Research Group, Faculty of Engineering and Environment, Northumbria University, Newcastle upon Tyne NE1 8ST, UK
[2]Department of Electromagnetic Field, Faculty of Electrical Engineering, Czech Technical University in Prague, 16627 Prague, Czech Republic
[3]Isocom Limited, 2 Fern Court, Bracken Hill Business Park, Peterlee, SR8 2RR, UK
*Corresponding author: zun.htay@northumbria.ac.uk

Received 24 March 2022; revised 23 June 2022; accepted 25 June 2022; published 14 July 2022

In this paper, we demonstrate the first, to our knowledge, experimental implementation of a gigabit Ethernet multiple input single output free space optical (FSO) communications link using adaptive switching implemented in the software defined open-source software, GNU Radio, and analyze its performance. A fully functional FSO link with a feedback path is implemented using cost effective off-the-shelf components, i.e., media converters and small form-factor pluggable modules. We propose a switching mechanism at the transmitter to improve the link performance under different fog conditions and provide results for the proposed FSO system compared with a single FSO link. The real-time channel estimation is demonstrated and, based on the channel state information, adaptive switching is carried out in GNU Radio. We show that the proposed system under the heavy fog condition offers almost the same packet error rate under the clear channel but with a reduced data rate by about 100 Mbps (i.e., 600 Mbps).

https://doi.org/10.1364/JOCN.458562

1. INTRODUCTION

The exponential growth of Internet of Things (IoT) devices has led to fine-grained traffic and spectrum utilization related issues that require novel wireless transmission solutions [1,2]. Over 70% of the global population is expected to have access to mobile connectivity by 2023 due to the greater access to devices such as smartphones, tablets, laptops, and recently deployed wearable connected devices [3]. Machine-to-machine connection followed by mobile connectivity is also projected to increase by 50% with 5.3 billion Internet users in 2023 [4]. The extraordinary advances are expected to be met in the fifth generation (5G), sixth generation (6G), and beyond due to the demands from the users. Additionally, it is expected that 5G will not be able to meet the market demands after 2030, where 6G technology is to fill the gap [5]. Note that 6G is not just an incremental upgrade but an exceptional leap in terms of data rates R_b, latency, reliability, security, and complexity. The ample number of innovations in telecommunications has been greatly contributed by the emerging technologies in different frequency bands such as millimeter wave, terahertz, optical fiber (OF), and optical wireless communications (OWC). These technologies are in the race to deliver fully automated intelligent networks, which require a high R_b with reliable connectivity for the revolution of 5G and 6G, and continuous developing standards to accommodate the demand. In both the "last mile" and "last meter" access networks, OWC is expected to be deployed alongside the radio frequency (RF) technology to ensure link availability under all weather conditions. OWC offers several advantages, such as a massive license-free spectrum (up to $\cong$ 400 THz, mostly at the infrared band) and therefore higher R_b, inherent security at the physical layer, and much reduced inter-channel interference compared with RF systems [6]. In OWC, free space optical (FSO) communications as a mature and well-developed technology has gained a substantial amount of interest in wireless front-haul access network applications [2,7]. In urban and built-up areas, where the deployment of cable-based fixed links is very costly, highly directional FSO systems utilizing the already available and well-developed components of long-distance matured OF communications technology can be rapidly deployed at low costs [8].

In FSO systems, link availability becomes a major issue due to its peculiar characteristic of being susceptible to atmospheric conditions [2]. Fog and turbulence contribute the most to the

degradation in the link performance by way of both amplitude (power) and phase fluctuation of the optical wavefront while propagating through the free space channel. To address the weather impact on the FSO link performance and ensure link availability at all times, techniques such as hybrid RF/FSO, multiple input multiple output (MIMO) FSO with spatial diversity (SD), and relayed FSO systems have been proposed in the literature [2]. Amongst the proposed solutions, SD techniques has been proven to perform better compared to the single FSO link in terms of bit error rate (BER) performance to mitigate the degradation due to the fog condition [9].

A comparative study of single input single output (SISO) and MIMO FSO systems under different weather conditions has been reported in the literature, showing that MIMO outperforms SISO in terms of the received power level and BER in [9–11]. Aside from MIMO and SD techniques, adaptive modulation and low-density parity-check coding for the SISO FSO system were proposed in [12], showing tolerance to a deep fade of the order of 30 dB and above under strong turbulence. A novel adaptive transmission algorithm for the optimization of both power usage and spectral efficiency for the satellite-to-ground communications with 10 dB of power-saving was proposed in [13]. In [9], a comparative analysis of a MIMO FSO link with adaptive switching to ensure link availability and SISO FSO under fog and turbulence conditions together with the investigation of the optimal threshold in terms of BER in a GNU Radio platform was reported. An analysis of an adaptive modulation FSO system with multiple apertures using the signal-to-noise ratio (SNR) threshold for dynamic adaptation of the modulation scheme was also reported in [14].

While there is a large body of literature on theoretical and simulation-based analysis on the optimization of FSO systems using adaptive algorithms, very little has been reported on the practical implementation of such systems. Most reported works in the literature are purely based on hardware solutions involving the use of traditional optical sources, photodetectors (PDs), and integrated circuit boards, which limit cross functionality and can only be modified through physical intervention. Even though there is a reconfigurable hardware solution involving the use of field programmable gate arrays (FPGAs) or digital signal processing (DSP) boards, it requires highly skilled and specialized personnel [15,16]. It is worth mentioning that software defined radio (SDR)-based platforms have been known to provide flexibility and reconfigurability in practical implementation and evaluation of adaptive techniques in MIMO FSO systems. Additionally, SDR, which is designed to remove hardware limitations, offers many advantages including (i) implementation of signal processing through the physical and medium access control layers [17], (ii) software-configurability and control, (iii) improved system performance with the efficient and flexible use of the RF spectrum for new services to the end users, (iv) a reduced system size and minimization of the design risk and time-to-market, and (v) flexibility in research and development due to the implementation and verification of a range of newly developed protocols [18]. The experimental implementation of SDR-based RF systems utilizing universal software radio peripheral (USRP) were reported in [19–21]. Highly flexible and powerful SDR platforms to accommodate 5G wireless networks have been reported in the literature [22] for the virtualization of SDR and software defined networking.

Although the SDR implementation of RF systems is rather common and well established, in OWC, we have also found some work on system implementation using various available software defined platforms including MATLAB, LabVIEW, GNU Radio, and so on for DSP and controlling the hardware. Experimental demonstration of a bidirectional visible light communication (VLC) system with adaptive modulation based on the noise, interference, and environmental impacts was proposed and investigated [23]. In [15], experimental evaluation and performance analysis of a VLC system were carried out using USRPs and LabVIEW software for audio streaming over a 1 m linkspan. An adaptive VLC system with adaptive software defined equalization techniques such as least mean squares, normalized least mean squares, and QR-decomposition-based recursive least-squares (QR-RLS) were analyzed in [24]. In [25], a commercially available OWC test kit [for both visible and infrared (IR) bands] with an SDR platform (i.e., compatible with LimeSDR USB and GNU Radio) for use in indoor, outdoor, and underwater communication applications with a transmission range over 20 m has been reported. Design and demonstration of the IR optical front end with a bandwidth of 10 MHz with USRPs was reported in [26], which was validated by the transmission of an audio signal. In [27], the advantages of implementing FSO systems based on SDR under different weather conditions to increase the link availability and reliability were investigated.

The reported works in the literature mainly utilized the LabVIEW software as the SDR ecosystem for control, test, and deployment of the system in real time. Alternatively, GNU Radio, which is a free and open-source software development toolkit, supports the real-time emulation to control and deploy the hardware using the time domain graphical user interface (GUI) [28]. We have reported the performance analysis of SDR-based MIMO and SISO FSO systems under different fog and turbulence conditions with adaptive switching in GNU Radio in [9]. However, the previous work is a real-time emulation system with a simulated FSO channel. In this work, we have (i) adopted GNU Radio to perform adaptive switching under different fog conditions in an experimental environment, which has not been reported before; (ii) demonstrated a real-time MIMO FSO system conforming with the gigabit Ethernet standard using cost-effective media converters and small form-factor pluggable (SFP) modules and analyzed the system performance of a 5 m long FSO link; (iii) designed and built out-of-tree (OOT) modules for the optical switch (OS) and the power meter to perform adaptive switching via a feedback link, from which the channel state information (CSI) is obtained; and (iv) developed the Python script, which is used for data generation and packet error rate (PER) testing.

We evaluate the proposed system under the heavy fog conditions and show that it offers much improved performance in terms of the PER, the standard deviation of the transmission delay of datagrams, jitter, and R_b compared with the single FSO link. To the best of the authors' knowledge, the proposed system is the first cost effective, off-the-shelf, gigabit Ethernet FSO link with the adaptive switching implemented in the SDR ecosystem domain. The rest of the paper is organized

as follows: Sections 2 and 3 describe the MIMO FSO system modeling and provide all the design considerations of the experimental demonstration and implementation of the adaptive switching mechanisms in the SDR/GNU-Radio environment. Section 4 explains the link budget analysis and delay compensation of the MIMO FSO system. Section 5 is devoted to the results and discussion on the measured data. Finally, Section 6 concludes the paper.

2. PROPOSED MIMO FSO SYSTEM

In the proposed system, two sets of transmitters (Txs) and receivers (Rxs) are used for parallel transmission of the same data to achieve 99.999% link reliability under fog conditions. Note that the link availability requirements generally depend on FSO deployment, i.e., in an enterprise or carrier network. For the former, the availability requirement of 99% is generally lower than the latter availability of 99.999% [29]. At the Tx side, a switching algorithm is proposed to switch on the additional Tx based on the CSI received via the feedback link, i.e., the visibility estimation (VE) laser FSO link. The considered key system parameters are given in Table 1. To assess the link performance, we consider three different fog conditions. The schematic diagram of the proposed MIMO FSO system with a feedback link is presented in Fig. 1. Link-1 is used for data transmission based on FSO, and Link-2 is based on fiber connection. Note that Link-2 can also be replaced by an FSO link. The Tx consists of a computer (i.e., Tx PC) as the client that can be considered as a data center for generating random data sequences, which is packetized and sent through the Python script. This script sends the user datagram protocol packets to the paired Python script acting as the server at the Rx PC. The Tx PC is connected via a LAN/Ethernet cable to the media converter (MC) to convert the 1 Gbps electrical signal into the optical domain using the fiber SFP transceiver module. The SFP output is applied to an optical coupler to split the incoming optical signal into two data streams for transmission over two single-mode fibers (SMFs). The first output of the coupler is applied to collimator 1 via a 3.25 m of SMF (a core diameter of 9 μm and at a wavelength λ of 1550 nm), which partially compensates for the delay of 16.2 ns due to the OS in the second parallel path. The second output of the coupler is applied to the OS and collimator 2. The collimator outputs are launched into the free space channel. Note that the OS is also connected to the Tx PC for adaptively switching Tx-2 based on the CSI. At the Rx, the incoming optical beams are captured using collimators 3 and 4, where the outputs are then combined using a 2 × 1 optical coupler. The coupler output is applied to the MC module via SFP to regenerate the electrical signal. The Rx PC is used to evaluate the link performance using the packet error rate tester (PERT) [30]. The VE laser used at the Rx is for estimating the fog attenuation/CSI experienced by the link. Using an optical power meter, the measured power of the received VE laser beam $P_{\mathrm{VE-Rx}}$ is applied to the power meter module in GNU Radio, the output of which is applied to the OS module. For the OS, we have adopted software-based Schmitt trigger thresholding based on the maximum measured received power of the VE laser. Note that, if $P_{\mathrm{VE-Rx}} < P_{\mathrm{VE-Lo}}$ (i.e., the lower limit of the received VE laser

Table 1. Key System Parameters

Parameter	Value
Link length l	5 m
Data throughput	1 Gbps
SFP output power P_{Tx}	∼4 dBm
Rx collimator diameter D_{Rx}	24 mm
Tx collimator diameter D_{Tx}	24 mm
Tx beam divergence θ	0.016°
Optical wavelength λ	1550 nm
SFP sensitivity	−23 dBm
Compensation delay SMF length	3.24 m
Collimator focal length f_l	37.13 mm
Tx and Rx separation distance d_{Tx} and d_{Rx}	∼8 cm

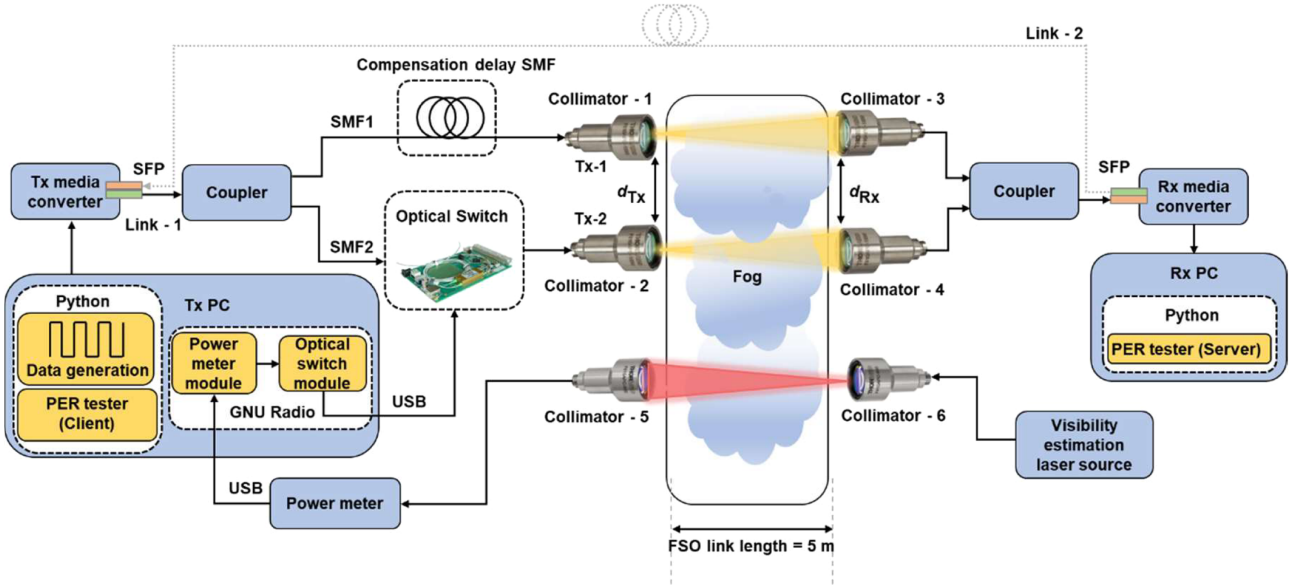

Fig. 1. Schematic system block diagram.

power) the Tx-2 is on, whereas for $P_{\mathrm{VE-Rx}} > P_{\mathrm{VE-Up}}$ (i.e., the upper limit of the received VE laser power) the Tx-2 is off and only the Tx-1 is on. The Schmitt trigger-based thresholding introduces hysteresis, and therefore different threshold levels are used to avoid unnecessary switching when the system is operating near the threshold level. The switching mechanism will ensure that the link availability is maintained as much as possible under all weather conditions at the cost of increased P_{Tx}.

(i) *Link power budget*—The received power can be expressed as a function of the transmitted power and the losses, which is given by

$$P_{\mathrm{Rx-Total}} = P_{\mathrm{Tx}} - L_{\mathrm{LC-\frac{FC}{APC}}} - 2L_{\mathrm{Cou}} + 10\log\left(10^{\frac{-L_{\mathrm{Delay}}}{10}} + 10^{\frac{-L_{\mathrm{OS}}}{10}}\right) - L_{\mathrm{Geo}} - L_{\mathrm{PE}}, \tag{1}$$

where $L_{\mathrm{LC-FC/APC}}$ and L_{Cou} are the LC-FC/APC connector loss and the loss due to the coupler. L_{Geo} and L_{PE} describe the geometric loss and the loss due to the pointing error. Due to the free space link length of 5 m and considering the specifications of the optics utilized in the setup, L_{Geo} and L_{PE} are neglected. L_{OS} and L_{Delay} are the losses at the delay line and the optical switch line, respectively, which can be expressed as

$$L_{\mathrm{Delay}} = 5L_{\mathrm{FC/APC}} + L_{\mathrm{Col-1}} + L_{\mathrm{Col-3}}, \tag{2}$$

$$L_{\mathrm{OS}} = 2L_{\mathrm{FC/APC}} + L_{\mathrm{Col-2}} + L_{\mathrm{Col-4}}, \tag{3}$$

where $L_{\mathrm{FC/APC}}$ is the FC/APC connector loss. $L_{\mathrm{Col-1}}$, $L_{\mathrm{Col-2}}$, $L_{\mathrm{Col-3}}$, and $L_{\mathrm{Col-4}}$ are the collimator losses. Table 2 shows the link budget analysis for both paths. To take care of any additional losses, including increased component losses and the received power fluctuation between a maximum of −4.6 dBm to a minimum of −12.9 dBm due to the coherent addition of the two optical waves and random phase shifts in between, we have considered the link margin of ∼10 dB.

(ii) *Channel*—We numerically determine the correlation length d_c and measure the separation space between Txs and Rxs, which must exceed $d_c \approx \sqrt{\lambda l}$, where l is the link length. The correlation coefficient $\rho = \exp\left(-\frac{d}{d_c}\right)$ [31] and the received signal is given by

$$y(t) = x(t)\Re\sum_{i=1}^{N_{\mathrm{Tx}}} I_i + n(t), \tag{4}$$

where $x(t)$ is the transmitted signal, $\Re$ is the photodetector responsivity, and $n(t)$ is the additive white Gaussian noise (AWGN) with variance σ_n^2. $I_i = -\gamma l I_o h_i$ is the received signal intensity from the ith Tx, where I_o is the received signal intensity for the ideal channel, h_i is the channel response, and l is the link distance. γ is the weather-dependent attenuation coefficient (in dB/km) typically 0.43 and 42.2 for clear air and moderate fog, respectively. For an FSO link, the channel gain due to the atmospheric conditions is defined by $h_a = e^{-\gamma l}$ [32]. The atmospheric attenuation is caused by the absorption and scattering due to aerosols and molecular components, which is expressed in terms of the attenuation coefficient as [1]

$$\gamma(\lambda) = \alpha_m(\lambda) + \alpha_a(\lambda) + \beta_m(\lambda) + \beta_a(\lambda), \tag{5}$$

where $\alpha_m(\lambda)$ and $\alpha_a(\lambda)$ are the molecular and aerosol absorption coefficients, respectively, and $\beta_m(\lambda)$ is the molecular scattering coefficient. The last term represents the aerosol scattering coefficient due to fog attenuation, which is used by the Tx switch unit in the proposed system and can be estimated using the following model [33]:

$$\beta_a(\lambda) = \frac{3.91}{V}\left(\frac{\lambda}{550\ \mathrm{nm}}\right)^{-q}, \tag{6}$$

where q is related to the size distribution of the scattering fog particles for which the Kim model is considered in this paper, as given by [34]

$$q = \begin{cases} 1.6 & V > 50\ \mathrm{km} \\ 1.3 & 6\ \mathrm{km} < V < 50\ \mathrm{km} \\ 0.16\,\mathrm{V} + 0.34 & 1\ \mathrm{km} < V < 6\ \mathrm{km} \\ V - 0.5 & 1\ \mathrm{km} < V < 1\ \mathrm{km} \\ 0 & V < 0.5\ \mathrm{km} \end{cases}. \tag{7}$$

In the proposed system, we estimated the scattering coefficient of the channel using Beer's law:

$$\beta_a(\lambda) = -\frac{\log\left(\frac{P_{\mathrm{VE-Rx}}}{P_{\mathrm{VE-Max}}}\right)}{l}, \tag{8}$$

where $P_{\mathrm{VE-Rx}}$ is the power received for the channel condition under evaluation and $P_{\mathrm{VE-Max}}$ is the maximum received power for a clear channel. The atmospheric loss is given by [35]

$$L_{\mathrm{Atm}}(\mathrm{dB}) = 4.343\beta_a(\lambda)l. \tag{9}$$

Table 2. Link Budget Analysis of a Combined Link

Parameter	Value	
	Path 1 (OS path)	Path 2 (Compensation delay path)
Transmit power P_{Tx}	0.25 dBm	0.25 dBm
Losses		
$L_{\mathrm{FC/APC}}$	0.35 dB	0.88 dB
$L_{\mathrm{LC-FC/APC}}$	0.15 dB	0.15 dB
L_{Cou}	3.75 dB	3.75 dB
$L_{\mathrm{Col-1}}$, $L_{\mathrm{Col-3}}$, $L_{\mathrm{Col-4}}$	0.5 dB	1.8 dB
$L_{\mathrm{Col-2}}$	3.6 dB	2.6 dB
Receiver sensitivity	−23 dBm	
Total average received power $P_{\mathrm{Rx-Avg}}$	−5.7 dBm	
Total minimum received power $P_{\mathrm{Rx-Min}}$	−12.9 dBm	
Link margin	10.1 dB	

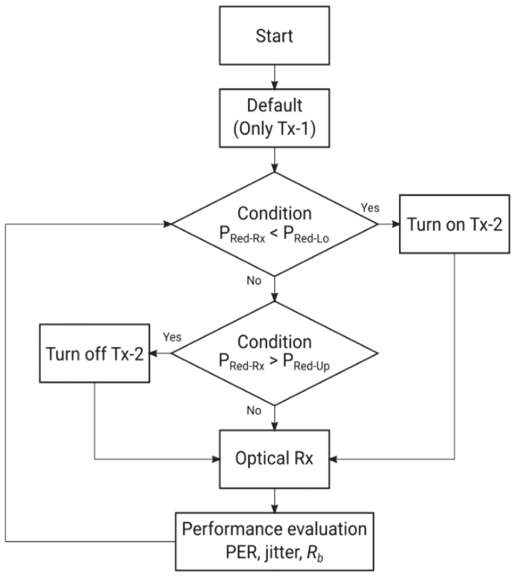

Fig. 2. System flowchart.

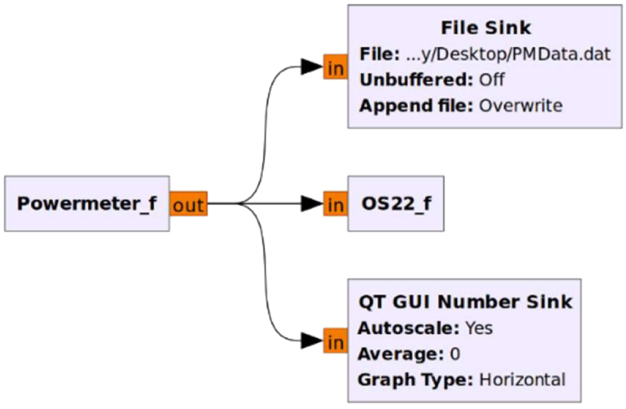

Fig. 3. OOT modules for the power meter and optical switch in the GNU Radio platform.

3. SOFTWARE AND HARDWARE IMPLEMENTATION

A. Adaptive Switching in the GNU Radio/SDR Platform and the FSO Link Performance Tester

To perform the proposed adaptive switching, we have implemented SDR-based decision-making blocks for the power meter and an optical switch in GNU Radio. GNU Radio can be used not only as a real-time simulation environment for DSP purposes but also to seamlessly integrate and control different hardware devices using Python language. Using the flowchart shown in Fig. 2, we have carried out a simulation to determine the PER, jitter, and R_b as a function of V for single FSO and MIMO FSO links with the length of 5 m in different fog conditions. Figure 3 shows the OOT modules for implementation of the power meter and OS in the GNU Radio domain. The measured power levels obtained from the Powermeter_f module are stored using the "File Sink" to determine the visibility using Eq. (8), which is then applied to the "QT GUI Number Sink" to display the information in real time, and the OS. In the OS we used two threshold levels of $P_{\mathrm{VE-Up}}$ and $P_{\mathrm{VE-Lo}}$, which are set to 0.275 and 0.225 mW, corresponding to the predicted L_{Atm} of 1.6 and 2.5 dB, respectively, for a single clear FSO link with $P_{\mathrm{VE-Max}}$ of 0.4 mW and a link margin of 8.6 dB. Considering L_{Atm}, the link margin before switching to path 2 is 6.1 dB. Therefore, we set the values of $P_{\mathrm{VE-Up}}$ and $P_{\mathrm{VE-Lo}}$ to ensure the link reliability. Note that the OS is controlled by the OS22 module. The OS22 block determines the OS states by using the Schmitt trigger thresholding method and the determined threshold values. We analyzed the performance of the proposed system using the developed Python tool based on *iperf*; see Fig. 4, which is an open source and commonly used network testing tool for (i) measuring the maximum achievable R_b, (ii) testing the system performance in terms of the PER and jitter, and (iii) measuring the end-to-end system throughput in one or both directions. For a back-to-back (B2B) link and under three different fog density conditions, we have measured the key parameters including $R_{b-\mathrm{Max}}$, jitter, and PER for 30 s each.

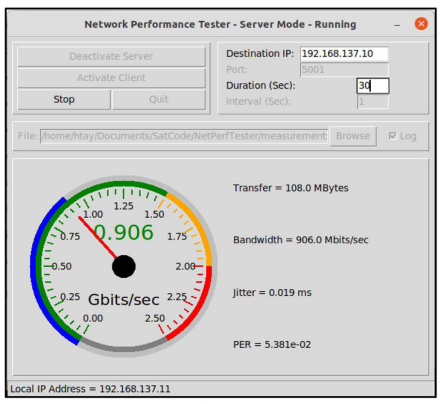

(a)

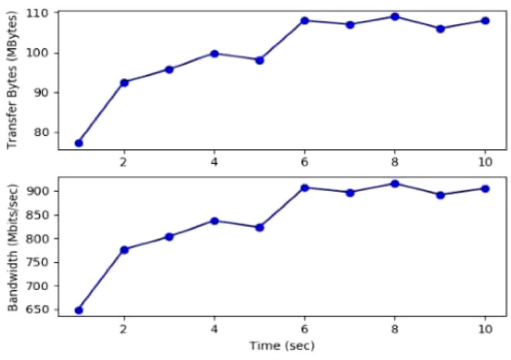

(b)

Fig. 4. Screenshots of the developed Python code for (a) the network performance tester for measuring the performance of the Ethernet FSO link and (b) the received data and bandwidth.

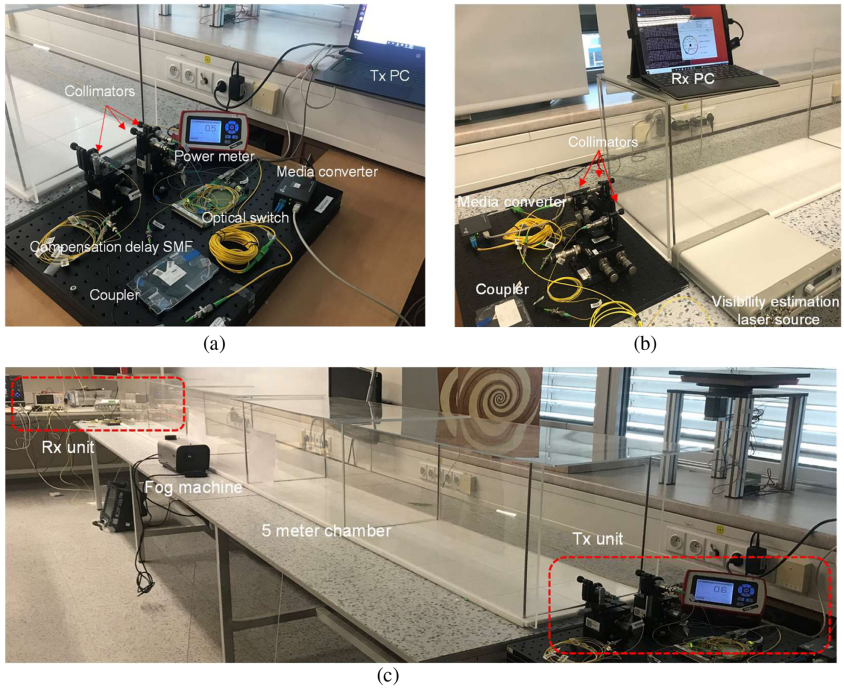

Fig. 5. Experimental setup of (a) a Tx with a PC connected to an MC to transmit data and a power meter to receive the VE laser and estimate the visibility. An optical switch is connected to the PC for adaptive switching according to the received CSI from the power meter. (b) Rx setup with the VE laser, two collimators for received signals, a coupler to combine two received signals, and an MC connected to the PC. (c) Channel setup when fog is injected.

B. Experimental Setup

We performed the measurements under different fog conditions and showed that the proposed system can effectively mitigate heavy fog over a 5 m link. Figure 4 shows the experimental testbed for the 1 Gbps MIMO FSO system with GNU Radio-based adaptive switching. The key system specifications adopted in the experimental setup are shown in Table 3. At the Tx, a PC is connected to the (i) power meter; (ii) OS via a USB cable; and (iii) SFP, which is integrated in the MC module via an Ethernet cable; see Fig. 5(a). A 1 Gbps non-return-to-zero on–off keying (NRZ-OOK) data output of the SFP is applied to the coupler via an SMF with its outputs connected to the compensation delay line and the OS feeding the Tx-1 and Tx-2 collimators. The use of the power meter is to estimate V of the channel using Eq. (6). As for the Rx, it consists of a visibility estimation laser source, collimators, SMF cables, and a 2×1 optical coupler; see Fig. 5(b). The output of the coupler is applied to the SFP MC module, which in turn is connected to the Rx PC. The generated optical signals are transmitted over a built indoor atmospheric chamber with the dimensions of $40 \times 40 \times 500$ cm^3; see Fig. 5(c).

Table 3. Component Specifications

Device	Specification
Media converter TP-Link MC220L)	IEEE 802.3ab, IEEE 802.3z, IEEE 802.3x
Small form factor pluggable module (SFP1000ZXST)	IEEE 802.3z 1000BASE-ZX Max data rate: 1.25 Gbps Max range: 80 kmSMF
Optical switch (OSW12-1310-E)	λ: 1280−1625 nm Switching rate: <1 ms SMF 75 dB (typical) Insertion loss: 0.7 dB
Power meter (PM100D-S120C)	λ: 400−1100 nm
Collimators 1–4 (F810APC–1550)	Effective f_l: 37.13 mm λ: 1550 nm
Collimators 5 and 6 (F810APC–842)	Effective f_l: 36.18 mm λ: 650−1050 nm
Coupler(s) (SC11C-002-0334 and 002-0354)	λ: 1310−1550 nm Split ratio: 50:50 Insertion loss: 3.5 dB SMF
(Red) laser source (MCLS1-CUSTOM)	λ: 638 nm Laser class: 3B
SMF delay line	Core diameter: 9 μm

4. EXPERIMENTAL RESULTS

The performance of the proposed MIMO FSO link with the adaptive switching algorithm implemented in the GNU Radio platform is investigated in this section. The objective has been to monitor and control the system operation in a real-time software domain. The implementation of the adaptive switching algorithm is based on the OOT blocks as outlined in Section 3.

We have carried out a set of tests and measurements for the three scenarios of B2B, SISO, and MIMO FSO under clear and foggy channel conditions. Note the following: we have (i) estimated V of 358 m for the clear channel and the obtained $P_{\mathrm{VE-Rx}}$ value and (ii) only considered the miscellaneous loss L_{misc} but not L_{Geo}, since it is negligible. Figure 6 depicts

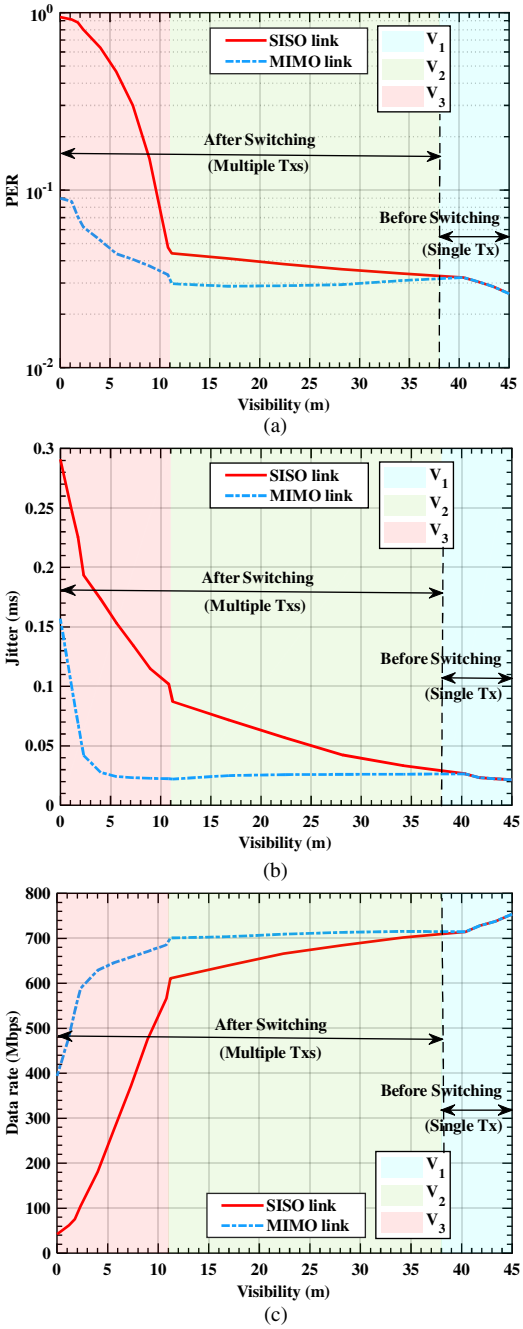

Fig. 6. Visibility versus (a) PER, (b) jitter, and (c) data rate for 5 m SISO and MIMO FSO links under fog conditions.

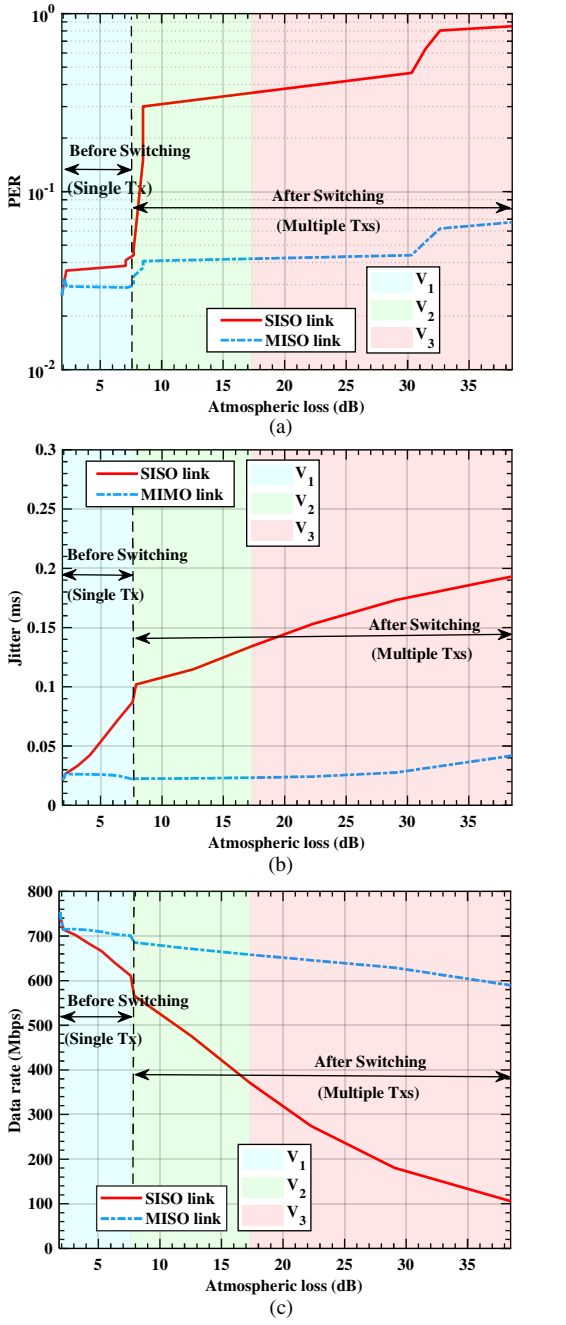

Fig. 7. Atmospheric loss versus (a) PER, (b) jitter, and (c) data rate for 5 m SISO and MIMO FSO links under fog conditions.

the plots for the PER, jitter, and R_b as the function of V for 5 m long SISO and MIMO FSO links. We have highlighted the three distinctive visibility ranges of $38 < V_1 < 45$ m, $11 < V_2 < 38$ m, and $0 < V_3 < 11$ m. As shown in Fig. 6(a), MIMO outperforms SISO in terms of the PER for V_1 and V_2. For $V < 38$ m, the PER of the SISO starts to increase, whereas for the MIMO link, the PER of 2×10^{-2} remains constant until a V of 11 m, which is due to turning on the additional Tx (i.e., the Tx-2). Beyond $V < 11$ m, the PER increases for both cases with MIMO showing a much lower rate of increment compared with SISO.

We observe that for $V < 5$ m, for SISO the PER is 0.55, which indicates link failure, whereas it is 4×10^{-2} for MIMO.

Note the same patterns for the jitter and R_b plots as illustrated in Figs. 6(b) and 6(c). In Fig. 6(b), for $V < 38$ m, the jitter increases almost exponentially for SISO, whereas for MIMO the rapid increase in the jitter is observed at $V < 5$ m. As for R_b it gradually decreases from ~ 700 to ~ 600 Mbps for V reduced from 38 to 11 m for SISO. This is because of the denser fog condition. However, for MIMO and the same V range, R_b of ~ 700 Mbps is maintained. Note that under more dense fog, R_b continues to decrease for both links beyond $V < 11$ m with MIMO offering much higher R_b compared

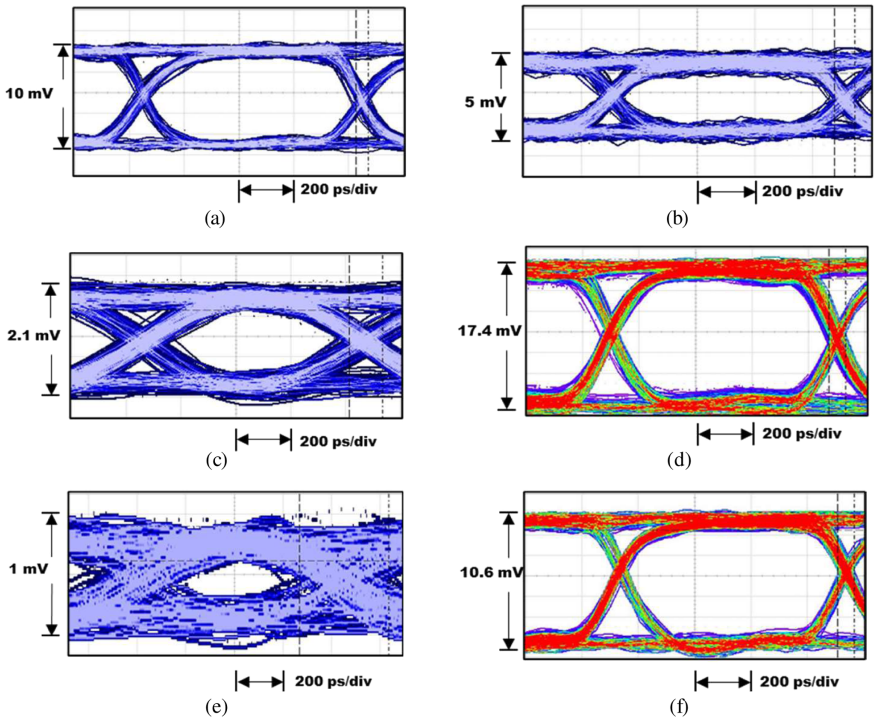

Fig. 8. Eye diagrams of the single FSO link: (a) under a clear channel, (b) V_1, (c) V_2, and (e) V_3. MIMO link for (d) V_2 and (f) V_3.

Table 4. Statistics of the System Performance Metrics for the B2B, Clear, and Increasing Fog Density Conditions of V_1, V_2, and V_3

Channel Condition	Parameter	Standard Deviation	Mean	Maximum	Minimum
B2B	PER	1.9×10^{-2}	2.1×10^{-2}	5.7×10^{-2}	2.2×10^{-6}
	R_b (Mbps)	78	846	929	612
	Jitter (ms)	8.6×10^{-6}	2.3×10^{-5}	3.5×10^{-5}	2×10^{-6}
Clear	PER	1.4×10^{-2}	2.9×10^{-2}	5.8×10^{-2}	1.1×10^{-3}
	R_b (Mbps)	81.3	703.8	845	543
	Jitter (ms)	4.4×10^{-6}	2.3×10^{-5}	3.7×10^{-5}	1×10^{-5}
V_1, $V \in (38, 45)$ m	PER	2.3×10^{-2}	3.3×10^{-2}	9.5×10^{-2}	1.7×10^{-3}
	R_b (Mbps)	126	643	803	426
	Jitter (ms)	1.1×10^{-4}	4.5×10^{-5}	2.2×10^{-4}	1.8×10^{-5}
V_2, $V \in (11, 38)$ m	PER	2.3×10^{-2}	4.1×10^{-2}	11.5×10^{-2}	4.6×10^{-3}
	R_b (Mbps)	118	630	802	404
	Jitter (ms)	1.8×10^{-4}	6.1×10^{-5}	4.2×10^{-4}	1.9×10^{-5}
V_3, $V < 11$ m	PER	7.2×10^{-2}	8.4×10^{-2}	29.7×10^{-2}	8.3×10^{-3}
	R_b (Mbps)	117	620.5	791	315
	Jitter (ms)	5.5×10^{-4}	8.5×10^{-5}	8.6×10^{-4}	2×10^{-5}

with SISO. We also provide Fig. 7, which indicates the same system performance in terms of L_{Atm} versus PER, jitter, and bandwidth. Figure 8 shows the measured eye diagrams for SISO and MIMO links for a range of V (i.e., fog conditions). Figures 8(a) and 8(b) depict the eye diagrams for SISO under clear and foggy channels (i.e., 38 m $< V_1 <$ 45 m), respectively, where the system is operating in the default state (i.e., using only the Tx-1). As expected, the best eye diagram with a wide eye opening is observed under the clear channel. Figures 8(c) and 8(e) show the eye diagrams for 11 m $< V_2 <$ 38 m and $0 < V_3 <$ 11 m, respectively, for the SISO FSO link. Figures 8(d) and 8(f) illustrate the eye diagrams for the MIMO system showing the effectiveness of adopting multiple Txs. In the clear channel, the maximum achievable R_b is 845 Mbps for a PER of 5.82×10^{-2}. Next, we performed measurements under fog conditions. Since the link margin of ~10 dB is sufficient to compensate for the fog-induced attenuation, MIMO is at the default state with noticeably reduced R_b of 643 Mbps and the jitter of 4.489×10^{-5} for the same PER of 2.3×10^{-2}. For 11 m $< V_2 <$ 38 m, the measured $R_{b-\max}$ is 630 Mbps for a PER of 4.06×10^{-2}. At this stage with $P_{\text{VE-Rx}} < P_{\text{VE-Lo}}$, the Tx-2 is switched on, i.e., the link is MIMO. Next, for 0 m $< V_3 <$ 11 m, we measured the PER, jitter, and $R_{b-\max}$ of 8.42×10^{-2}, 8.54×10^{-5} ms, and 620.5 Mbps, respectively, compared to SISO with the PER, jitter, and R_b of 0.8, 2×10^{-4} ms, and 84.9 Mbps, respectively.

In addition, we carried out a set of tests and measurements using an *iperf*-based FSO performance tester for the B2B link and the clear and foggy channels with the results displayed in Table 4. It is noticed that the behavior of the switching mechanism does not depend on V but on the atmospheric attenuation and therefore the link length. Finally, we also considered longer link lengths of 500 m, 1 km, and 2 km with the same atmospheric losses for practical applications and theoretically enumerated that V of 1, 2, and 4 km are the points of switching, respectively. Furthermore, we have obtained a similar improvement in system performance under fog conditions compared to previous work in [9,36].

5. CONCLUSION

In this paper, we experimentally demonstrated a real-time gigabit Ethernet MIMO FSO link together with the implementation of adaptive switching in the GNU Radio platform and investigated its performance under different fog conditions. We analyzed the system using the developed FSO performance tester and discussed the important parameters of the system such as the PER, jitter, and data rate. We showed that the proposed MIMO FSO with adaptive switching mitigates the effects of heavy fog much more effectively with almost the same performance as SISO under a clear channel. Furthermore, we showed that the proposed MIMO FSO link experienced a reduced data rate of <400 Mbps and the increased jitter and PER of >0.15 ms and 10^{-1}, respectively, for $0\ \text{m} < V_3 < 11$ m. Finally, we concluded that (i) MIMO with the synchronized parallel transmission can effectively mitigate the fog-induced losses, while a small delay (nanosecond, ns) can cause an oscillation in amplitude when two parallel signals are combined; (ii) the randomness of the fog attenuation can cause amplitude fluctuations in the results; and (iii) implementing adaptive algorithms in GNU Radio provides a high degree of flexibility in the design and implementation of SDR-based systems.

Funding. Isocom; Intensive Industrial Innovation Program Northeast (25R17P01847); European Regional Development Fund; European Union COST Action CA19111 NEWFOCUS and CTU (SGS20/166/OHK3/3T/13).

Acknowledgment. We thank the CTU Laboratory for the use of their equipment.

REFERENCES

1. M. Uysal, C. Capsoni, Z. Ghassemlooy, A. Boucouvalas, and E. Udvary, *Optical Wireless Communications: An Emerging Technology*, 1st ed., Signals and Communication Technology (Springer, 2016).
2. A. K. Majumdar, Z. Ghassemlooy, and A. A. B. Raj, *Principles and Applications of Free Space Optical Communications* (2019).
3. M. Uysal, "Visible light communications: from theory to industrial standardization," in *Optical Fiber Communication Conference (OFC)*, 3–7 March 2019, paper Th3I.4.
4. Cisco, "Cisco Annual Internet Report (2018–2023) White Paper" (9 March 2020).
5. M. Z. Chowdhury, M. Shahjalal, S. Ahmed, and Y. M. Jang, "6G wireless communication systems: applications, requirements, technologies, challenges, and research directions," IEEE Open J. Commun. Soc. **1**, 957–975 (2020).
6. M. M. Abadi, Z. Ghassemlooy, N. Mohan, S. Zvanovec, M. R. Bhatnagar, and R. Hudson, "Implementation and evaluation of a gigabit Ethernet FSO link for 'the last metre and last mile access network'," in *IEEE International Conference on Communications Workshops (ICC Workshops)*, 20–24 May 2019.
7. Z. Ghassemlooy, W. Popoola, and S. Rajbhandari, *Optical Wireless Communications: System and Channel Modelling with MATLAB* (CRC Press/Taylor & Francis Group, 2019).
8. A. Abdalla, J. Rodriguez, I. Elfergani, and A. Teixeira, *Optical and Wireless Convergence for 5G Networks* (2019).
9. Z. Htay, Z. Ghassemlooy, M. M. Abadi, A. Burton, N. Mohan, and S. Zvanovec, "Performance analysis and software-defined implementation of real-time MIMO FSO with adaptive switching in GNU radio platform," IEEE Access **9**, 92168–92177 (2021).
10. M. Eghbal and J. Abouei, "Performance improvement of MIMO FSO systems against destructive interference," IET Commun. **13**, 2923–2931 (2019).
11. S. M. Moustafa, H. A. Fayed, M. H. Aly, and M. Mahmoud, "SISO and MIMO FSO based links under different weather conditions: system evaluation," Opt. Quantum Electron. **53**, 674 (2021).
12. I. B. Djordjevic, "Adaptive modulation and coding for free-space optical channels," J. Opt. Commun. Netw. **2**, 221–229 (2010).
13. M. Karimi and M. Uysal, "Novel adaptive transmission algorithms for free-space optical links," IEEE Trans. Commun. **60**, 3808–3815 (2012).
14. H. Nouri and M. Uysal, "Adaptive free space optical communication system with multiple apertures," in *24th Signal Processing and Communication Application Conference (SIU)*, 16–19 May 2016, pp. 937–940.
15. W. Hussain, H. F. Ugurdag, and M. Uysal, "Software defined VLC system: implementation and performance evaluation," in *4th International Workshop on Optical Wireless Communications (IWOW)*, 7–8 September 2015, pp. 117–121.
16. O. Hiari and R. Mesleh, "A reconfigurable SDR transmitter platform architecture for space modulation MIMO techniques," IEEE Access **5**, 24214–24228 (2017).
17. R. Verdecia-Peña and J. I. Alonso, "A comparative experimental study of MIMO A&F and D&F relay nodes using a software-defined radio platform," Electronics **10**, 570 (2021).
18. X. Li, W. Hu, H. Yousefi'zadeh, and A. Qureshi, "A case study of a MIMO SDR implementation," in *IEEE Military Communications Conference (MILCOM)*, 16–19 November 2008.
19. H. B. Thameur and I. Dayoub, "SDR implementation of a real-time testbed for spectrum sensing under MIMO time-selective channels for cognitive radio applications," IEEE Sens. Lett. **5**, 7002704 (2021).
20. S. Galih, M. Hoffmann, and T. Kaiser, "Low cost implementation for synchronization in distributed multi antenna using USRP/GNU-radio," in *1st International Conference on Information Technology, Computer, and Electrical Engineering*, 8 November 2014, pp. 457–460.
21. D. Stanko, G. Sommerkorn, A. Ihlow, and G. D. Galdo, "Enable software-defined radios for real-time MIMO channel sounding," in *IEEE International Instrumentation and Measurement Technology Conference (I2MTC)*, 17–20 May 2021.
22. H. Feng, J. Wu, and X. Gong, "SOUP: advanced SDR platform for 5G communication," in *IEEE/CIC International Conference on Communications in China (ICCC)*, 22–24 October 2017.
23. A. Costanzo, V. Loscri, and M. Biagi, "Adaptive modulation control for visible light communication systems," J. Lightwave Technol. **39**, 2780–2789 (2021).
24. R. Martinek, L. Danys, and R. Jaros, "Adaptive software defined equalization techniques for indoor visible light communication," Sensors **20**, 1618 (2020).
25. Hyperion Technologies, "LiFi R&D kit" [accessed 17 November 2020], http://www.hyperiontechs.com/lifi-rd-kit/.
26. H. Boeglen, S. Joumessi-Demeffo, S. Sahuguede, P. Combeau, D. Sauveron, and A. Julien-Vergonjanne, *Optical Front-Ends for USRP Radios* (2018).
27. A. Gruber, S. S. Muhammad, and E. Leitgeb, "A software defined free space optics (SD-FSO) platform based on an analog optical

frontend," in *Proceedings of the 11th International Conference on Telecommunications*, 15–17 June 2011, pp. 363–366.
28. GNU Radio, "About GNU Radio" [Accessed 2021], https://www.gnuradio.org/about/.
29. I. Kim and E. Korevaar, "Availability of free-space optics (FSO) and hybrid FSO/RF systems," Proc. SPIE **4530**, 84–95 (2001).
30. M. M. Abadi, "NetPerfTester" [Accessed 2021], https://github.com/MansourM61/NetPerfTester.
31. M. Abaza, R. Mesleh, A. Mansour, and E. M. Aggoune, "Spatial diversity for FSO communication systems over atmospheric turbulence channels," in *IEEE Wireless Communications and Networking Conference (WCNC)*, 6–9 April 2014, pp. 382–387.
32. E. Leitgeb, S. S. Muhammad, C. Chlestil, M. Gebhart, and U. Birnbacher, "Reliability of FSO links in next generation optical networks," in *Proceedings of 7th International Conference Transparent Optical Networks*, 7 July 2005, Vol. **1**, pp. 394–401.
33. M. K. El-Nayal, M. M. Aly, H. A. Fayed, and R. A. AbdelRassoul, "Adaptive free space optic system based on visibility detector to overcome atmospheric attenuation," Results Phys. **14**, 102392 (2019).
34. P. W. Kruse, L. D. McGlauchlin, and R. B. McQuistan, *Elements of Infrared Technology: Generation, Transmission, and Detection* (1963).
35. R. Paudel, Z. Ghassemlooy, H. Le-Minh, and S. Rajbhandari, "Modelling of free space optical link for ground-to-train communications using a Gaussian source," IET Optoelectron. **7**, 1–8 (2013).
36. M. Singh, "Mitigating the effects of fog attenuation in FSO communication link using multiple transceivers and EDFA," J. Opt. Commun. **38**, 169–174 (2017).

Zun Htay received a B.Eng. degree in electrical and electronics engineering from Northumbria University, Newcastle upon Tyne, UK, in July 2019, where she is currently pursuing a Ph.D. with the Optical Communications Research Group (OCRG). Her main research interests include free space optical communications, software defined systems, and near infrared laser communications. During her bachelor's degree, she received the Most Outstanding Student of the Department Award by IET and awarded by IEEE for her final year project poster presentation. Her Ph.D. is fully funded by the Intensive Industrial Innovation Program Northeast (IIIP NE), UK, and is partly funded by the European Regional Development Fund (ERDF) and ISOCOM Ltd.

Carlos Guerra Yánez received his M.Eng. degree in 2021 from Universidad de Las Palmas de Gran Canaria, Spain. He is currently a Ph.D. student in the Wireless and Fiber Optics group at the Czech Technical University in Prague, Czech Republic. His current research interests include signal processing, modulation techniques, and channel coding for visible light communications as well as quantum key distribution over free space optics.

Professor Zabih Ghassemlooy (Fellow, Optica; Fellow, IET; Senior Member, IEEE; Member, ACM), CEng, has 18,393 Google Scholar Citations and a Google Scholar h-index of 58 and i10-index of 368. He received his B.Sc. (Hons.) from Manchester Metropolitan University, UK, in 1981 and his M.Sc. in 1984 and his Ph.D. in 1987 from Manchester University, UK. During 1987–1988 he was a Postdoctoral Research Fellow at City University, UK. During 1988–2004 he was at Sheffield Hallam University, UK. During 2004–2014 he was the Associate Dean for Research, Faculty of Engineering and Environment, at Northumbria University, UK. He is currently the Head of the Optical Communications Research Group (one of the largest groups in optical wireless communications in Europe). He was a Research Fellow (2016) and a Distinguished Professor (2015) at the Chinese Academy of Science and a Visiting Professor at the University of Tun Hussein Onn Malaysia (2013–2017); Huaqiao University, China (2017–2018); the Technical University of Prague, Czech Republic (2019); and the Technical University of Graz, Austria (2018). He was the Vice-Chair of EU Cost-Action IC1101 (2011–2016) and is the Vice-Chair of Cost Action CA19111, 2020–2024. He has over 970 publications [410 journals (IEEE, IET, IoP, Optica, Elsevier, etc.) and 8 books], has given over 110 keynote/invited talks, and has supervised 11 Research Fellows and 71 Ph.D.s. His research interests include optical wireless communications (OWC), free space optics, visible light communications, optical camera communications, and hybrid RF-OWC, with many funded research projects from the Research Council (UK), UK Space Agency, European Union, and industries in collaboration with many international research centers. He has been leading the European Collaborative Research Network since 2020. He is the Chief Editor of the *British Journal of Applied Science and Technology* and the *International Journal of Optics and Applications*, Associate Editor of several journals (IEEE, IET, etc.), and Co-guest Editor of many special issues on OWC. He is the Vice-Chair of the Optica Technical Group on Optics in Digital Systems (since 2018) and the Chair of the IEEE Student-Branch at Northumbria University (since 2019). During 2004–2006 he was the IEEE UK/IR Communications Chapter Secretary. He has also been Vice-Chair (2006–2008), Chair (2008–2011), and Chair of the IET Northumbria Network (2011–2015). He is the founder and chair of the IEEE/IET International Symposium on Communications Systems, Networks and DSP; West Asian Symposium on Optical and mmW Wireless Communications; and South American Colloquium on Visible Light Communications as well as co-founder of several international events including the Workshop on Optical Wireless Communications at IEEE ICC since 2015, the colloquium on OWC at CSNDSP since 2004, and the international Workshop on OWC since 2015. He is a member of the international technical committee of a very large number of international conferences..

Stanislav Zvanovec received his M.Sc. and Ph.D. degrees from the Faculty of Electrical Engineering, Czech Technical University (CTU) in Prague, in 2002 and 2006, respectively. He is currently working as a Full Professor, the Deputy Head of the Department of Electromagnetic Field and head of Wireless and Fiber Optics at CTU (optics.elmag.org). His current research interests include free space optical, visible light communications, and fiber optical systems; OLED-based technologies; and RF over optics. He is the author of two books (and co-author of *Visible Light Communications: Theory and Applications*), several book chapters, and more than 300 journal articles and conference papers.

Mojtaba Mansour Abadi received a B.Sc. degree in electrical engineering from Islamic Azad University, Fasa, Iran, in 2005, and a M.Sc. degree in electromagnetic fields and waves from the K. N. Toosi University of Technology, Tehran, Iran, in 2008. In 2016, he received his Ph.D. in optical communication from the optical communications research group (OCRG), Northumbria University, Newcastle upon Tyne, UK. He is currently a lecturer in the Mathematics, Physics, and Electrical Engineering Department at Northumbria University. His research interest is mainly focused on optical devices, optics, electronics and optics prototyping, terrestrial optical communications, and space optical communications.

Andrew Burton received his B.Eng. (Hons.), M.Sc., and Ph.D. degrees from the Faculty of Engineering and Environment, Northumbria University, Newcastle UK in 2007, 2008, and 2015, respectively. Following the Ph.D., he served as a postdoctoral researcher with the renowned Optical Communications Research Group (OCRG) working with organic LEDs for optical communications. He has published over 50 scholarly articles in the field of optical communications, with the majority in upper quartile publications. He is currently the technical manager at Isocom Ltd., where they build and test opto-electronic components for the space, military, and commercial sectors. His research interests are focused on optical communications, digital signal processing, and opto-electronic systems.